

CHARACTERIZING CHAIN SCISSION IN AQUEOUS POLYMER SOLUTIONS

2.1 Introduction

Aqueous Sprays in Agriculture

In an agricultural setting, water-based sprays feature prominently, from irrigation of crops to application of relevant chemicals, such as fertilizers and pesticides. Substantial amounts of chemicals intended for crop leaves have off-target landing sites, such as on plants in other fields, on the soil, or on local wildlife.^{1,2} Groundwater and well-water contamination by pesticides is a significant and pervasive long-term health and environmental hazard, in addition to consequences of acute exposure.³⁻⁶

Spray-based application of chemicals faces two major challenges related to droplet size. Fine droplets (typically defined as having diameters in the range 50-200 μm) may drift on the wind away from the intended crops.^{7,8} Large droplets may rebound or roll off leaf surfaces (particularly an issue for hydrophobic, angled leaves, such as those of corn).^{1,2,9,10} Controlling both droplet size and deposition behavior is desirable to mitigate these challenges.¹¹⁻¹³ Additive candidates include surfactants (outside the scope of this work) and polymers, along with other surface tension and rheological modifiers. As discussed in detail in Chapter 1, polymers have a substantial effect on droplet average size, distribution of sizes, and impact, motivating study of water-soluble polymers with large effective sizes in solution as additives in agricultural applications.^{7,9,11,14-16}

Current implementation of polymer additives in agricultural settings is limited

by efficacy in field-relevant settings. Commercially available long water-soluble homopolymers, such as poly(ethylene oxide), suffer from significant degradation when undergoing pumping.^{7,17-19} Due to this vulnerability to scission, these long polymers lose efficacy in their performance as mist control and drag reduction agents as their effective size decreases.^{7,11,15,20}

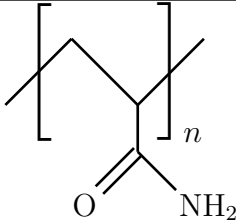

To combat degradation, our group has designed aqueous end-associative polymers to reversibly form supramolecular moieties, with synthesis conducted by Hojin Kim and characterization conducted by Hojin Kim and Robert Learsch. To establish an upper bound on the unit length for these end-associative polymers and better understand the threshold for chain scission, I compared homopolymers of two different water-soluble backbones, poly(ethylene oxide) (PEO, widely available and studied) and polyacrylamide (PAM, the backbone for the end-associative polymers). In addition to establishing guidelines for how long the unimers can be for a pumping-tolerant additive, understanding how chain scission impacts the extensional properties, and thus expected effects on the application relevant behavior, is key to designing additives that are tolerant to varying application conditions and bounding the range of outcomes if an additive system is mishandled, either in storage or use.

Comparing Properties of Polyacrylamide and Poly(ethylene oxide)

Though both water-soluble polymers, the anticipated changes to the extensional flow, and thus to chain scission, due to PAM versus PEO were not immediately apparent due to inconsistencies and gaps in literature data on PAM in water. Relevant properties of the two backbones are discussed below and summarized in Table 2.1.

When an application is limited by polymer additive loading by mass, minimizing molecular weight per backbone atom is one metric for increasing the

Table 2.1: Structure and properties of polyacrylamide (PAM) and poly(ethylene oxide) (PEO).

	polyacrylamide (PAM)	poly(ethylene oxide) (PEO)
structure		
molecular weight per backbone atom (g/mol/BBA)	35.5	14.7
Kuhn-Mark- Houwink-Sakurada Exponent in Water (<i>a</i>)	0.62-0.8 ²¹⁻²³	0.68-0.78 ^{24,25}
characteristic ratio	8.5 ²⁶ 12.7 ²⁷	6.7 ²⁸ 6.9 ²⁷
chain scission force (nN) ²⁹	4.38 ± 0.16	2.30 ± 0.22
backbone bond theoretical strength (nN) ²⁹	4.1 (C-C)	4.1 (C-C) 4.3 (C-O)

effective length of a polymer additive at a particular weight concentration. PEO has all heavy atoms in the backbone, leading to a molecular weight per backbone atom (BBA) of 14.7 g/mol/BBA, while PAM is heavier, at 35.5 g/mol/BBA, due the side groups on the backbone.

In addition to differences in length due to proportion of atoms in the backbone to side groups, effective size at equilibrium is modified by the solvent quality of the backbone (see discussion of the Kuhn-Mark-Houwink-Sakurada equation and the relationship to the Flory exponent in Chapter 1). Literature data for PAM is relatively sparse, with disagreement about the value of the exponent

indicating solvent quality (a in Equation 1.2), ranging from 0.62-0.8 for PAM in water at 30 °C over a similar range of molecular weights.²¹⁻²³ Literature on PEO in water is more available, although with some disagreement on the value of a —at similar temperatures to those studied for PAM, a is reported in the range 0.68-0.78.^{24,25} Further comparison of Kuhn-Mark-Houwink-Sakurada exponents across literature sources for PAM and PEO appears in Table 2.3 in the Results section. The expansion of the chain is both due to interactions with the solvent and due to the chain’s self-interactions and steric hinderance. PAM’s side groups prevent the chain from adopting an ideal chain configuration at small length scales, leading to a higher mean square end-to-end distance at equilibrium for the same number of backbone bonds than PEO.^{26,27} Available characteristic ratio values for each backbone are reported in Table 2.1.

Prior work comparing the behavior of PAM and PEO indicated that PEO undergoes chain scission at lower force on the backbone than PAM. Vanapalli, et al. used drag force scaling from turbulent flow at the Kolmogorov scale to calculate the maximum force a backbone can survive, given the weight-average molecular weight achieved at steady state after repeated chain scission (Equation 2.1).²⁹

$$F_{max} = A^{3/2} \frac{\pi \eta_{solv} Re^{3/2} L^2}{4 \rho d^2 \ln(L/a_d)} \quad (2.1)$$

A is an order 1 factor based on the geometry, which Vanapalli et al. assumed to be 1 in calculations of the bond strength. η_{solv} is the solvent viscosity. $Re = \frac{\rho U d}{\eta_{solv}}$ is the Reynolds number, ρ is the fluid density, U is the mean velocity, and d is the dimension of the geometry. L is the contour length of the chain. a_d is the chain diameter. Based on the body of literature of chain scission data for which laminar scaling does not correspond, Vanapalli, et al.’s estimations of the force for scission of PEO was 2.30 ± 0.22 nN and for PAM was 4.38 ± 0.16 nN, assuming a chain diameter of 1 nm.²⁹ Incorporating

differences in chain diameter due to PAM's bulky side groups compared to PEO into their calculation would further amplify this difference between PAM and PEO, implying that we should expect PAM to resist chain scission up to a higher force compared to PEO, although with the trade-off of increased drag on PAM's backbone.

Based on the above survey of properties of homopolymer PAM and PEO, PAM is expected to have a smaller effect on shear and extensional properties per unit mass and that PEO is expected to degrade more significantly in chain scission events.

Extensional Rheology of Polyacrylamide and Poly(ethylene oxide)

To contextualize results in this study, a brief survey of literature results for the extensional rheology and implications for mist control applications of PAM and PEO is included below. More discussion on chain scission can be found in Chapter 1. Further discussion of PAM and PEO as drag reducing agents and the degradation that occurs in turbulent flow experiments can be found in Chapter 3.

The extensional properties of PEO have been correlated with modification of droplet formation during spraying¹⁶ and retention upon impact,^{2,9,30} although the precise mechanism for retention has been contested (further discussion in Chapter 1).^{14,31,32} At relatively low loadings by mass (<0.1 wt %), long PEO (>1 Mg/mol) dissolved in water has been shown to suppressing small (satellite) droplets in sprays¹⁶ and prevent droplet rebound from both synthetic and plant hydrophobic surfaces.^{2,9,30} These studies highlighted the resistance to extension or stretching of the polymer chain as the primary modifier of the solution behavior.^{9,16}

Although PEO is a potent mist control and droplet retention agent in the lab,

chain scission inhibits practical applications in the field.^{7,17–19} To characterize chain scission, degradation studies have typically looked at relationships between extension rate and molecular weight at scission, with the underlying mechanism hypothesized to be the extensional forces exceeding the polymer’s ability to dissipate energy through conformation changes—if the polymer is fully extended, the critical extensional rate would be inversely related to the extensional relaxation time.^{33–35} The extensional properties, however, of weakly viscoelastic solutions of relatively low solvent viscosities, such as low concentrations of PEO and PAM in water, were historically difficult to measure quantitatively.³⁶ Many studies of degradation of PEO primarily focused on the semi-dilute regime.^{37,38} Prior studies of dilute solutions indirectly probed extensional properties, for example, by measuring pressure drop during flow through a packed bed^{20,39} or by using opposing jets, for which substantial empirical corrections must be applied, even in the Newtonian case.³⁰

Tools to directly measure the extensional properties of highly dilute solutions in low viscosity solvents (such as water) have only been developed in recent years—dripping-onto-substrate extensional rheometry (DoSER)³⁶ and Rayleigh Ohnesorge jetting extensional rheometry (ROJER)¹⁶ enable extensional studies of solutions with relaxation times and viscosities below what is accessible in traditional capillary-breakup extensional rheometry (CaBER)⁴⁰ and microfluidic instruments.^{37,38} The methodology of DoSER is described in detail in Chapter 1.

Recent extensional results using DoSER and ROJER utilized PEO as a baseline for comparison to other viscoelastic materials.^{16,36,41–45} Aqueous, dilute PEO solutions demonstrated concentration-dependent behavior in extensional flow well below the overlap concentration,^{36,43} further supporting hypotheses of chain-chain interaction in extensional flow even when the solution is suf-

ficiently dilute at equilibrium conditions.⁴⁶ Direct comparisons of PAM and PEO solutions are sparse—comparing results of semi-dilute solutions of PEO and PAM in glycerol/water mixtures from different sources demonstrates similar relaxation times for similar ranges of shear viscosity; however, variations in glycerol/water ratios prevents quantitative analysis of differences^{42,47}

In this work, I considered the relative solvent quality of PAM and PEO at the temperature of our chain scission and extensional experiments. To account for differences in relative swelling of the chains, solutions used in chain scission were prepared at the same reduced concentration. I used dripping-onto-substrate extensional rheology to track the degradation of PAM and PEO homopolymers dissolved in water during pumping, and compared to direct measurements of molecular weight using gel permeation chromatography.

2.2 Experimental Methods

Materials

Polyacrylamide (PAM) was prepared by Hojin Kim. PAM synthetic details to be included in the thesis of Hojin Kim. Low dispersity poly(ethylene oxide) (PEO) acquired from Agilent. High dispersity PEO was acquired from multiple sources as noted in Table 2.2. Table 2.2 includes number-average molecular weight (M_n), weight-average molecular weight (M_w), dispersity (\mathcal{D}), and source for each polymer used in this chapter.

Solution Preparation

Solutions for Kuhn-Mark-Houwink-Sakurada (KMHS) intrinsic viscosity measurements were prepared by dissolving polymer in deionized water (DI water), rolling for a minimum of overnight (for polymers of molecular weights less than 50 kg/mol) to a maximum of one week (for polymers with molecular weights greater than 1 Mg/mol) at 10 rotations per minute (rpm). Stock solutions

Table 2.2: Molecular weights, dispersities, and sources for polyacrylamide (PAM) and poly(ethylene oxide) (PEO) samples.

Backbone	M_w (Mg/mol)	M_n (Mg/mol)	D	Usage	Sample Name	Source
PAM	0.18	0.17	1.0	KMHS		HK
PAM	0.49	0.48	1.0	KMHS		HK
PAM	0.75	0.73	1.0	KMHS		HK
PAM	1.65	1.50	1.1	KMHS		HK
PAM	2.34	1.40	1.7	KMHS		HK
PAM	4.19	3.21	1.3	CS	4M PAM	HK
PAM	4.80	3.00	1.6	KMHS		HK
PAM	6.70	5.00	1.3	KMHS, CS	6.7M PAM	HK
PEO	0.02	0.02	1.1	KHMS		Agilent
PEO	0.10	0.09	1.1	KHMS		Agilent
PEO	0.27	0.25	1.0	KHMS		Agilent
PEO	0.49	0.21	2.3	OC		Aldrich
PEO	0.97	0.87	1.1	KHMS	1M PEO	Agilent
PEO	1.38	1.14	1.2	KHMS		Agilent
PEO	1.40	0.38	3.7	OC		Dow WSRN12K
PEO	2.00	0.42	4.8	OC		Aldrich
PEO	2.10	0.98	2.1	OC		Aldrich
PEO	6.00	3.80	1.6	OC, CS	6M PEO	Dow WSR301

M_w : Weight-average molecular weight, M_n : Number-average molecular weight,

D: Dispersity index (M_w/M_n)

PAM: Polyacrylamide, PEO: Poly(ethylene oxide),

KMHS: Kuhn-Mark-Houwink-Sakurada (Figures 2.1 and 2.2),

OC: Overlap concentration (Figure 2.2),

CS: Chain scission (Figures 2.3-2.8),

HK: Hojin Kim.

were then diluted with DI water to appropriate concentrations and allowed to roll for a minimum of overnight.

Solutions for chain scission were prepared by dissolving polymer in deionized water at 0.38 times or 0.16 times the overlap concentration determined through KMHS measurements, as appropriate, and allowed to roll for a week at 10 rpm. Solutions prepared at 0.38 times the overlap concentration were divided in two, with one portion used for chain scission experiments immediately and one portion further diluted to 0.19 times the overlap concentration and allowed to roll overnight before chain scission experiments.

Chain Scission

I collected aliquots of the as-prepared solutions, and after 1, 5, 10, and 20 passes through the pump for analysis with DoSER and GPC. PAM solutions for $c/c^* = 0.16$ and all 6M PEO solutions were run on the same pump. To prevent cross-contamination, a new separate pump was used for PAM solutions for the experiments for $c/c^* = 0.19$ and 0.38. Each pump was washed with soap and water, thoroughly rinsed with deionized water, and allowed to dry between the solutions. The pump model used in all experiments was a 20W Imagitarium Aquarium Powerhead, with an operating speed of 303 gal/hour.

Shear Rheological Measurements

Shear viscosity measurements were performed on an Anton Paar MCR 302 WESP rheometer using a cone-and-plate fixture of 50 mm diameter and 2.007° angle, with a truncation of 0.207 mm. Solutions were loaded by depositing 1.1 mL of the solution on the center of the plate, lowering the cone to 0.217 mm, removing excess to create a flat edge, and then lowering to 0.207 mm to create a spherical edge condition. The plate was cooled to $15 \pm 0.1^\circ\text{C}$ using a Peltier plate to regulate temperature and match ambient conditions experienced in

extensional rheology. Solutions were allowed to thermally equilibrate and relax for 5 min. Shear rate sweeps were performed from 1 to 100 1/s. The solution edge was examined to check for evidence of evaporation and none was observed.

Dripping-onto-Substrate Extensional Rheometry (DoSER)

A dripping-onto-substrate extensional rheometry (DoSER) instrument was constructed by Robert Learsch and Red Lhota consisting of a GSVitec MultiLED G8 with QT lamp head (12000 lumen light source, Figure 1.7A), a Harvard Elite 11 syringe pump on an adjustable track (solution delivery, **B**), Photron FASTCAM Nova S12 type 1000K-M-32GB (high-speed camera, **C**) equipped with an optical train as described below, and a custom holder for aluminum substrates (**D**). The optical train consisted of a Resolve4K 7:1 Zoom Video microscope lens, two rear projection lenses, a 1.0x objective lens, and a coupler, resulting in a resolution limit at full zoom of 3.5 μm (**E**). The camera was operated at 25,000 frames per second with a shutter speed of 150,000 Hz (i.e., 7 μs exposure). The light passes through a diffuser before reaching the measurement plane (**F**).

A syringe with a 22G blunt-tip stainless-steel needle (outer diameter 0.718 mm) was mounted to the syringe pump. The substrate was positioned at a height of 2.8 mm below the tip of the needle, corresponding to a height-to-needle-diameter ratio of 4 or a height-to-initial-droplet-diameter ratio of 1, which is within the optimal range for water solutions.⁴⁸ Ambient temperature was measured with each experiment and was in the range 15 ± 1 °C.

For each solution, DoSER was performed using the following procedure. An aliquot was slowly loaded into a syringe through a 22G stainless-steel blunt-tip needle. The syringe was attached to the syringe pump and the syringe pump was slowly advanced until solution was observed to drip from the needle, and

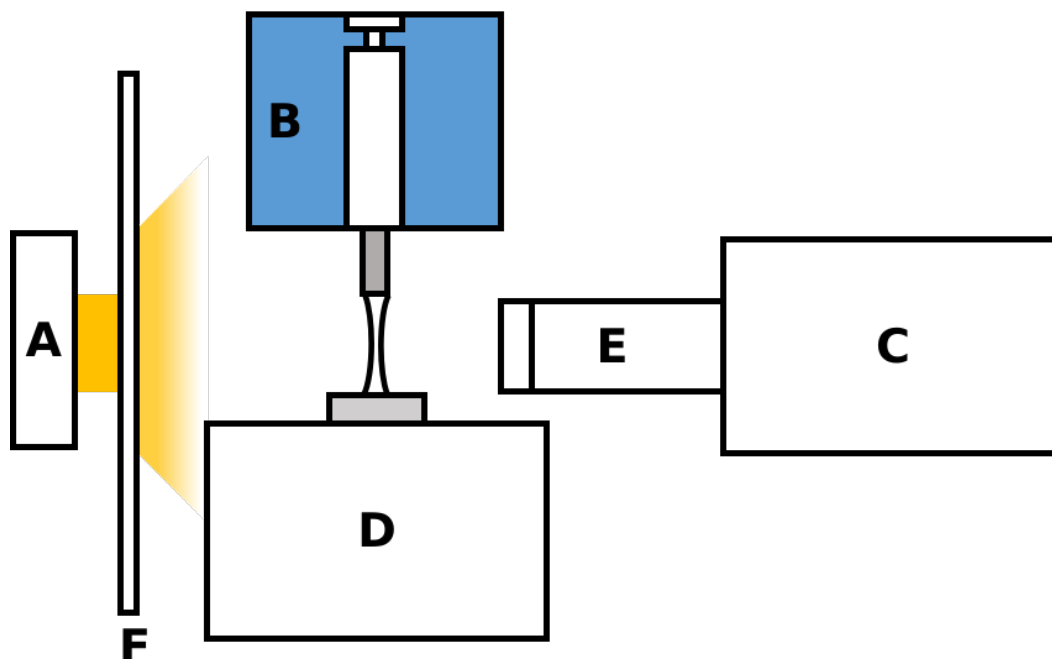


Figure 1.7: Schematic of dripping-onto-substrate extensional rheometer (not to scale). (repeated from page 14)

then the needle tip was cleaned. A clean set of aluminum substrates was loaded onto the substrate holder and the first substrate was aligned below the needle tip. The light was turned on and the camera was focused and aligned with the needle tip. The substrate was then raised or lowered to the correct height (as describe above) relative to the needle tip. A background video with a droplet-free needle and substrate was acquired. A drop was dispensed from the needle tip by the syringe pump at a rate of 0.02 mL/min, until the drop was nearly touching the substrate. The syringe pump was stopped prior to droplet-substrate contact. The events of droplet contact through liquid bridge formation and pinchoff were recorded (referred to as an experimental video or “run”). A clean substrate was then placed below the needle tip. Dispensing drops onto a clean substrate was repeated until five total runs were recorded. The videos were analyzed using the *dosertools* Python package, described in detail in Appendix A, to obtain the normalized diameter as function of time

after the critical time (time of transition between solvent behavior and elasto-capillary response). The decay of the normalized diameter is used to evaluate the extensional relaxation time. In our experiments, run-to-run variation on the DoSER instrument was observed to be more significant than errors in fitting—errors in measured relaxation times are thus quantified using the run-to-run variation. Solutions with relaxation times of 0.05 ms and lower were difficult to consistently characterize on our instrument.

Further discussions of DoSER theory and analysis are available in Chapter 1 and Appendix A respectively.

Gel Permeation Chromatography

Aliquots collected pre- and post-pumping were diluted using DI water to sufficiently low concentrations for characterization with aqueous gel permeation chromatography (GPC). PEO solutions were diluted to 0.0025 wt % or lower. PAM solutions were diluted to 0.02 wt % or lower. Solutions were passed through a 0.45 μm syringe filter after dilution.

The molecular weights and dispersity index of the polymers in solution were determined on a GPC system with an Agilent PL Aquagel-OH Mixed-H 8 μm 300 x 7.5mm column, Wyatt DAWN 8 multi-angle laser light scattering detector ($\lambda=658.9\text{nm}$), and a Waters Optilab differential refractometer (RI) ($\lambda=658\text{nm}$). Water with 200 ppm sodium azide and 8.5 g/L sodium nitrate was used as the eluent at the flow rate of 0.3mL/min with a temperature of 25°C. The data were analyzed using Wyatt Astra Software (version 7.3.2.19) using the Zimm fitting formula with $dn/dc = 0.136 \text{ mL/g}$ for PEO and $dn/dc = 0.159 \text{ mL/g}$ for PAM in water to obtain the weight-average molecular weight (M_w) for each polymer reported.

Characterizing high molecular weight poly(ethylene oxide) aqueous solutions

Backbone	Temperature (°C)	$K * 10^4$ (1/wt %)	a	Source
PAM	15	4.3	0.61 ± 0.04	This study
PEO	15	3.2	0.70 ± 0.06	This study
PAM	30	0.63	0.8	Scholtan (1954) ²¹
PAM	30	6.8	0.66	Collinson, et al. (1957) ²²
PAM	30	0.65	0.62	Misra, et al. (1979) ²³
PEO	15	5.0	0.68	Gregory, et al. (1986) ²⁴
PEO	30	1.2	0.78	Bailey, et al. (1958) ²⁵

Table 2.3: Kuhn-Mark-Houwink-Sakurada prefactor (K) and exponent (a) (Equation 1.2) for polyacrylamide and poly(ethylene oxide) in water.²¹⁻²⁵ ($a \pm$ one standard deviation, K standard deviations were less than 10^{-8})

via gel phase chromatography (GPC) can be challenging due to column interactions and polymer aggregation. PEO with weight-average molecular weight can be well-characterized up to 2.5 Mg/mol and PAM up to 5 Mg/mol.⁴⁹

2.3 Results

Comparisons in Solvent Quality

Intrinsic viscosity as a function of weight-average molecular weight was compared to available literature values for Kuhn-Mark-Houwink-Sakurada coefficients for PAM and PEO (Figure 2.1, Table 2.3). Logarithmic fits of the Kuhn-Mark-Houwink-Sakurada equation (Equation 1.2) to the measured data produced $K = 4.3 * 10^{-4}$ (1/wt %) and $a = 0.61 \pm 0.04$ for PAM and $K = 3.2 * 10^{-4}$ (1/wt %) and $a = 0.70 \pm 0.06$ for PEO ($a \pm$ one standard deviation, K standard deviations were less than 10^{-8}).

The overlap concentration was calculated from the intrinsic viscosities measured using Equation 1.1 (Figure 2.2). High dispersity ($M_w/M_n > 1.3$) PEO samples were also characterized in addition to PAM and the low dispersity ($M_w/M_n < 1.3$) PEO samples shown in Figure 2.1. The weight-average num-

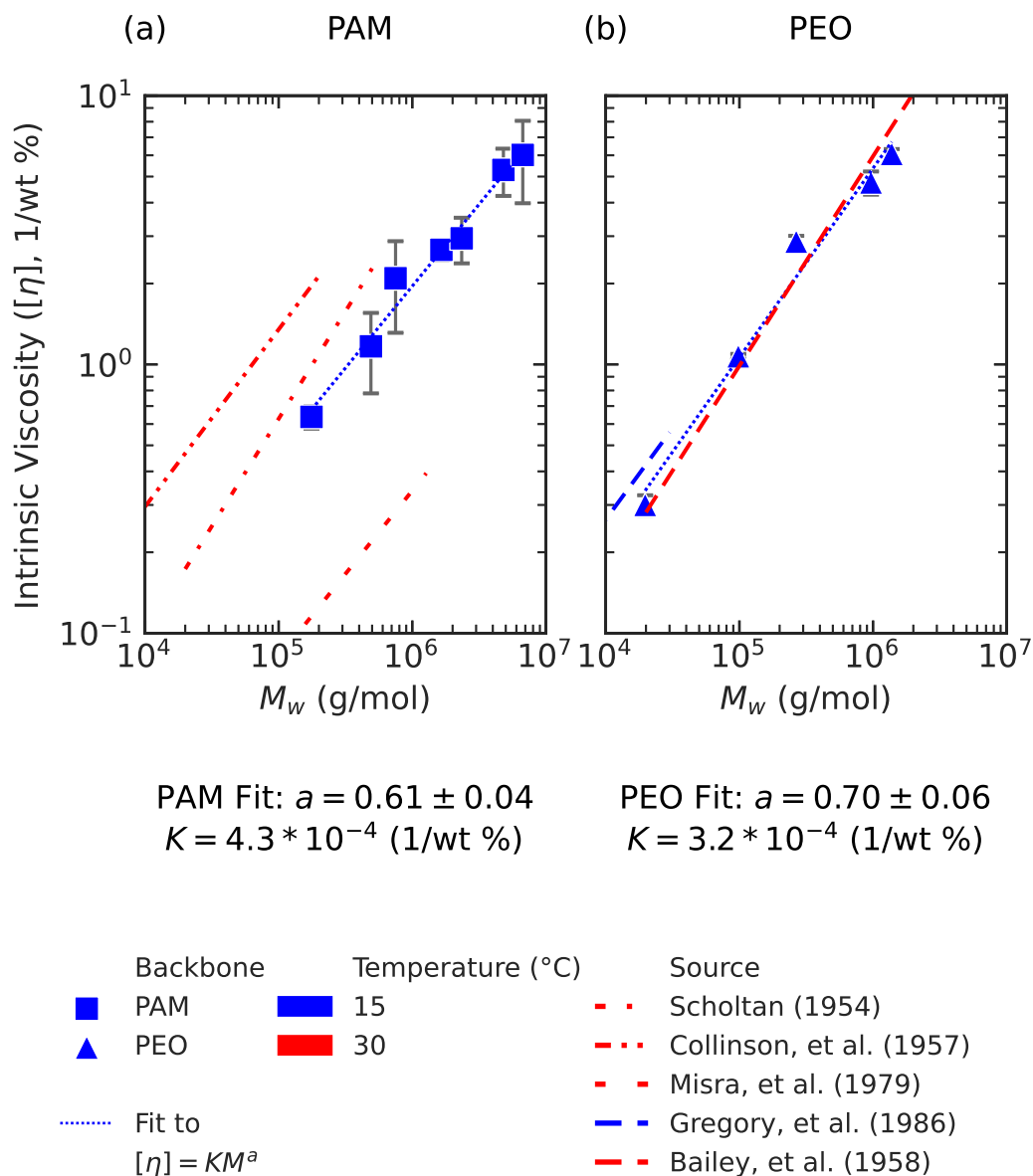


Figure 2.1: Intrinsic viscosity ($[\eta]$, 1/wt %) as a function of weight-average molecular weight (M_w , g/mol) for (a) polyacrylamide (PAM) and (b) poly(ethylene oxide) (PEO) at 15°C. Kuhn-Mark-Houwink-Sakurada (KMHS) fits to experimental results (blue dotted line) are (a) $K = 4.3 * 10^{-4}$ (1/wt %) and $a = 0.61 \pm 0.04$ for PAM, and (b) $K = 3.2 * 10^{-4}$ (1/wt %) and $a = 0.70 \pm 0.06$ for PEO. Error bars indicate 95% confidence interval. Where error bars are not visible, 95% confidence interval is within the symbol size. Comparison to literature KMHS values at 15 °C (where available) and 30 °C are presented over their stated valid molecular weight ranges (Table 2.3).²¹⁻²⁵

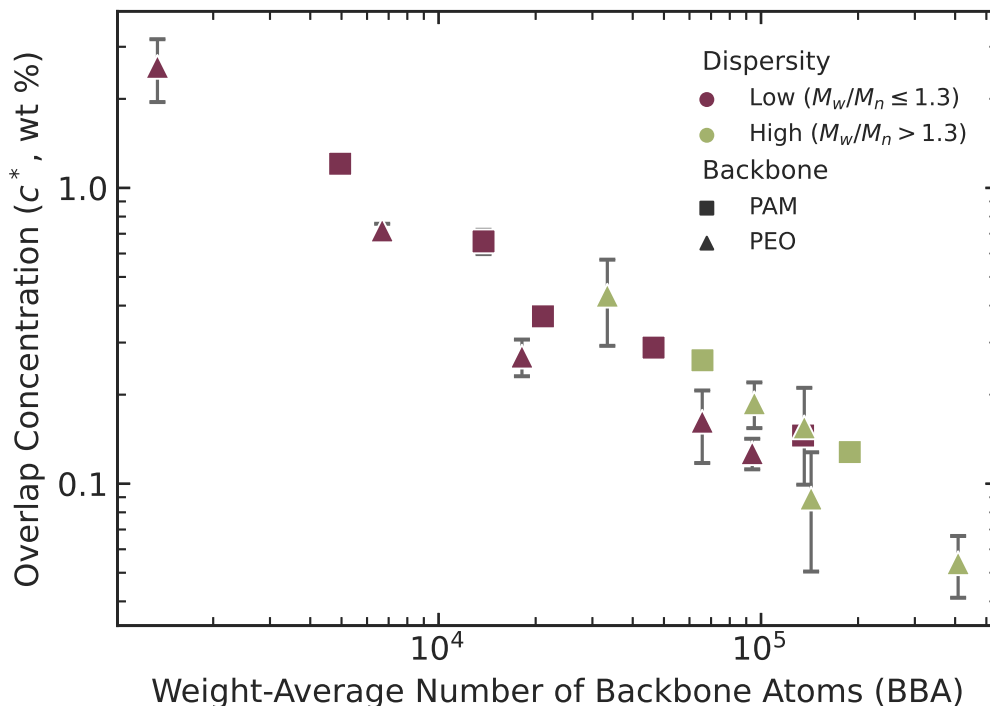


Figure 2.2: Overlap concentration (c^* , wt %) as a function of weight-average number of backbone atoms (BBA) for low dispersity PAM and low ($M_w/M_n \leq 1.3$) and high ($M_w/M_n > 1.3$) dispersity PEO at 15 °C.

ber of backbone bonds was calculated by taking the weight-average molecular weight divided by the repeat unit molecular weight and multiplied by the number of backbone bonds per repeat unit (Equation 2.2).

$$n_{w,backbone\ bonds} = M_w \frac{n_{backbone\ bonds\ per\ repeat\ unit}}{M_{repeat\ unit}} \quad (2.2)$$

Measurement of Degradation Using GPC

PAM and PEO samples with similar number of Kuhn steps were chosen for chain scission experiments—4M PAM, ($N_k \approx 9,000$) and 1M PEO ($N_k \approx 9,000$)—along with a high molecular weight PEO (6M PEO, Dow WSR301, $N_k \approx 55,000$) also observed to undergo chain scission in turbulent flow (see Chapter 3). Samples of as-prepared solutions and aliquots taken after selected numbers of passes through a centrifugal pump were analyzed using gel permeation chro-

matography (GPC) with refractive index (RI) and multi-angle light scattering (MALLS) detectors. ASTRA software (Wyatt Technologies) was used to analyze the elution curves (Figure 2.3(a)) and evaluate the number- and weight-average molecular weights (M_n and M_w). The highly disperse 6M PEO presented a number of challenges: 1) the measured mass recovery of these samples was low ($\sim 50\%$), indicating loss of sample to the column, which precludes reliable molecular weight determination by GPC results, and 2) “spikes” in the 6M PEO chromatograms (red arrows in Figure 2.3(a)) indicated aggregates or particulates with higher signal than those reliably measurable in our instrument, despite injecting the filtered samples at very low concentrations.

Ratios of measured molecular weight ($M_{w,i}$) to starting molecular weight ($M_{w,0}$) were calculated at pass $i = 1, 5, 10,$ and 20 for two different concentrations ($c/c^* = 0.19$ and 0.38) (Figure 2.3(b)). Thus, there are two symbols for each sample at each number of passes. Where only one symbol is visible, $M_{w,i}$ were indistinguishable for the two concentrations. By inspection of the GPC traces and analysis through ASTRA of the corresponding refractive index measurements, very little change occurs in the first pass for all samples but 6M PEO at $c/c^* = 0.38$. Accordingly, those five values of $M_{w,1}/M_{w,0} \approx 1$. Likewise, by inspection, there is no significant change in the GPC traces of 1M PEO for up to 20 passes for both concentrations (middle of Figure 2.3(a)); so $M_{w,i}/M_{w,0} \approx 1$ for all i for 1M PEO. The first sample to show significant reduction of M_w is 6M PEO: $M_{w,5}/M_{w,0} \approx 0.65$ for both concentrations tested, and the GPC traces show a decrease in the population of the longest chains (those that elute within 19 minutes). Note that 1M PEO does not contain such long chains in its distribution. After 10 passes, degradation becomes measurable in 4M PAM and continues for 6M PEO; both 4M PAM and 6M PEO show small further

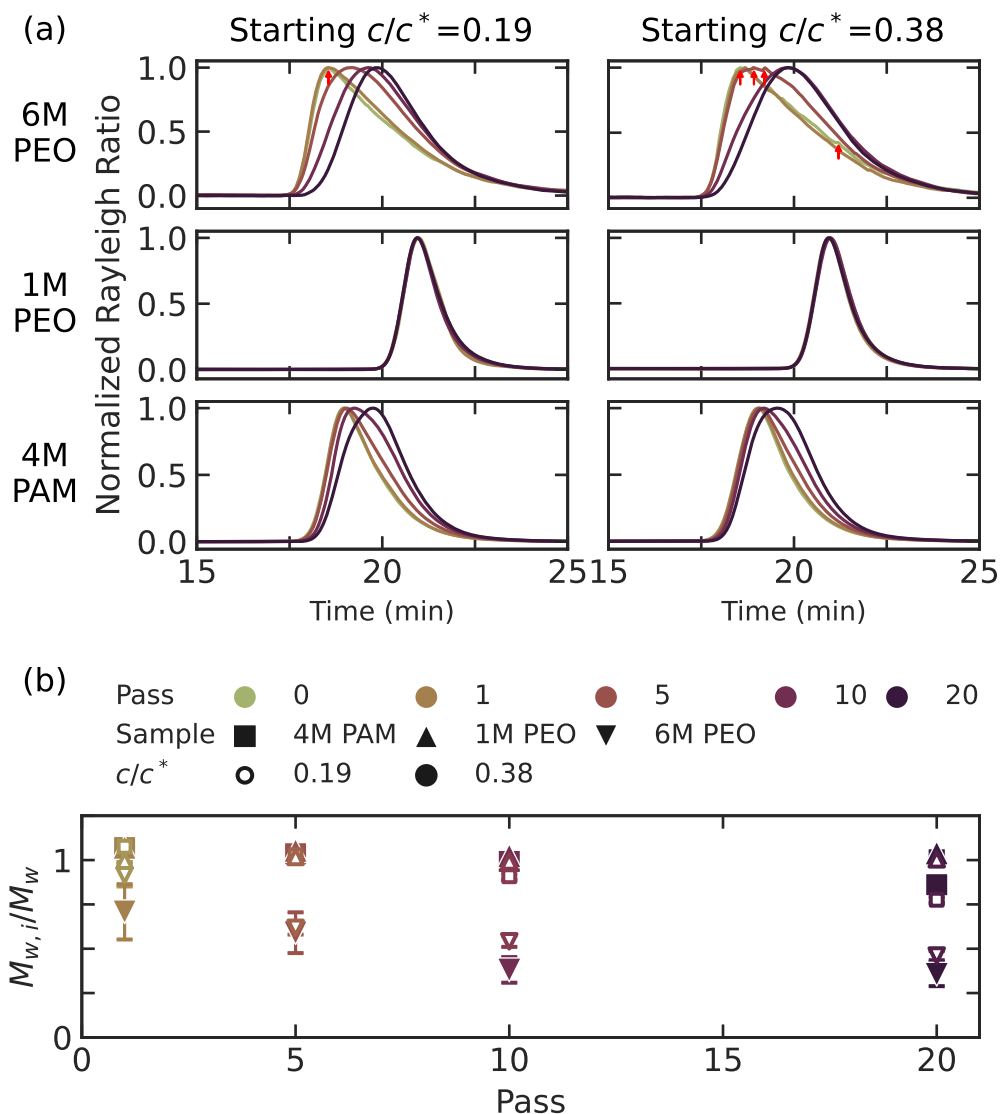
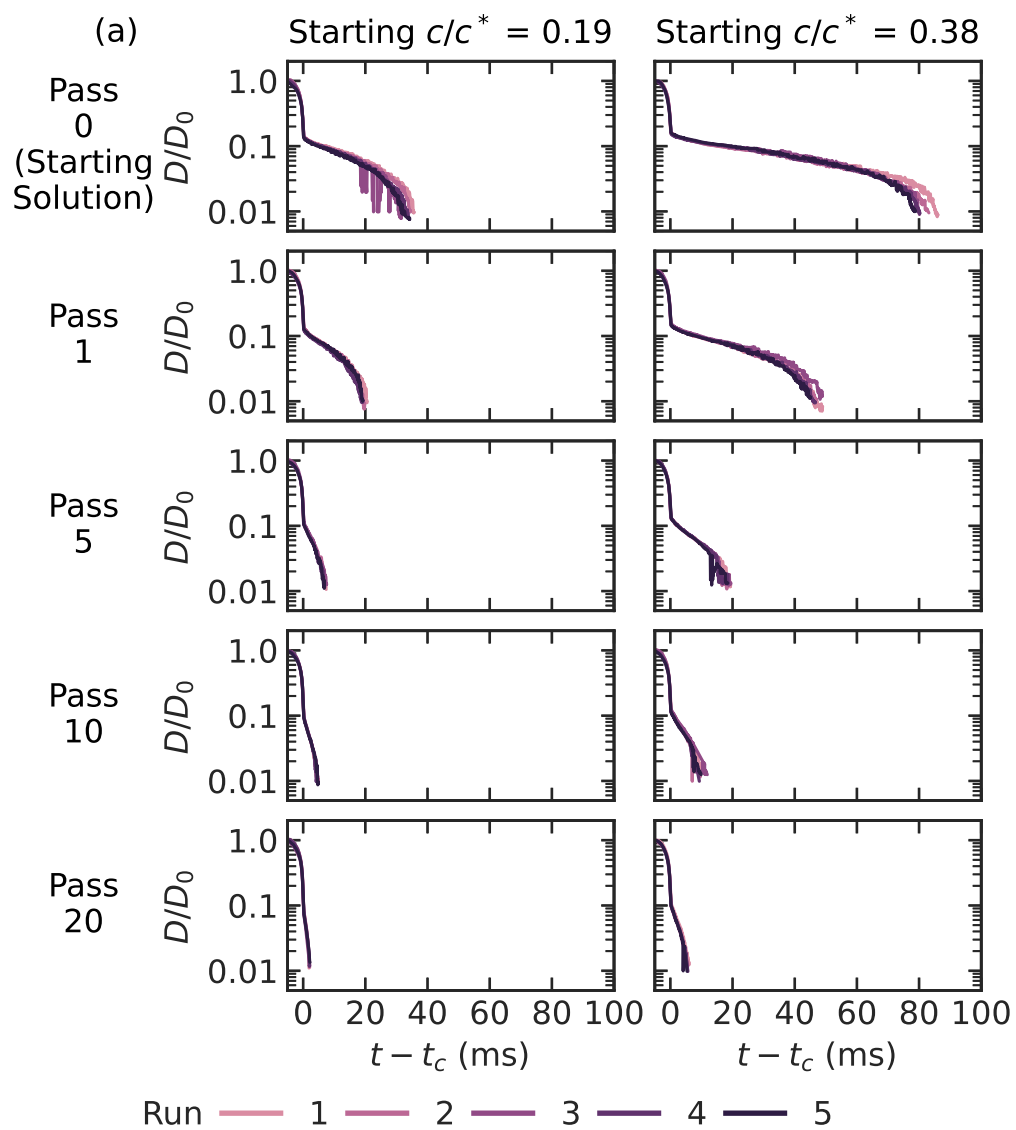


Figure 2.3: (a) Normalized Rayleigh Ratio as a function of aqueous gel permeation chromatography elution time (min) for samples with starting molecular weights and backbones of 4M PAM, 1M PEO, and 6M PEO, after 0, 1, 5, 10, and 20 passes through a pump at a concentration of c/c^* of 0.19 (left) and 0.38 (right). (b) Ratio of measured weight-average molecular weight M_w ($M_{w,i}$) at pass $i = 1, 5, 10,$ and 20 to starting M_w ($M_{w,0}$) as a function of pass for samples shown in (a). Error bars represent the statistical standard deviation from propagation of uncertainty of weight-average molecular weight as determined in ASTRA GPC software. Where error bars are not visible, standard deviation is within symbol size. Reported ratios for 6M PEO samples should be treated as estimates (see text for details).

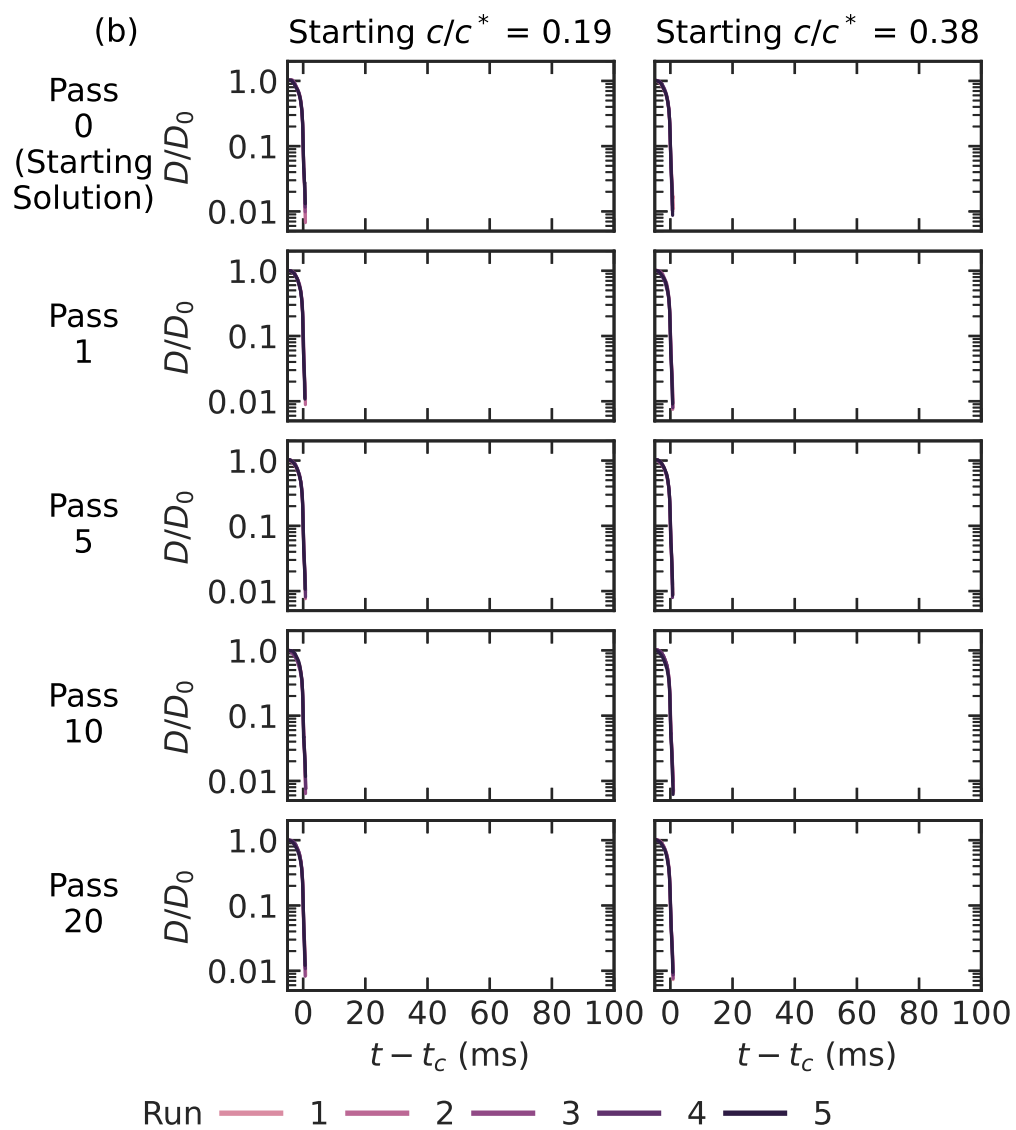
shift in M_w from 10 to 20 passes.

Measurement of Degradation using Extensional Rheology

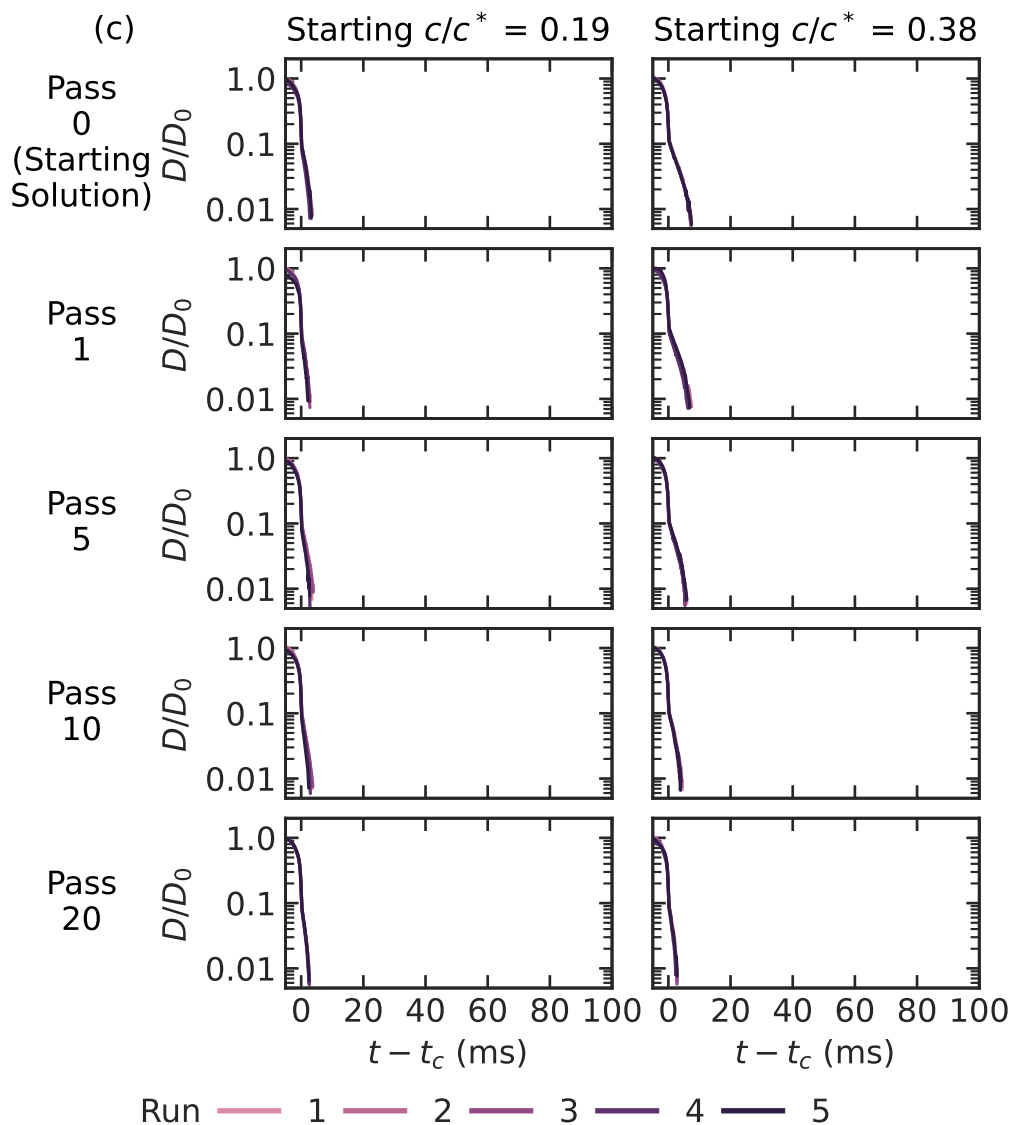
Normalized diameter (D/D_0) was measured by image analysis of high-speed videos of dripping-onto-substrate extensional rheometry experiments and the critical time was evaluated from $D(t)/D_0$ as described in Appendix A (Figure 2.4). The inertio-capillary regime (times less than the critical time) appeared very similar across samples, and is consistent with water-only observations (Figure 2.5). The duration of the elastocapillary (EC) regime differed among samples, with the longest observable EC regime seen in the as-prepared 6M PEO solution at the higher concentration ($c/c^* = 0.38$), and the shortest EC regime seen in the 1M PEO solutions at the lower concentration ($c/c^* = 0.19$).



(a) 6M PEO, $c/c^* = 0.19$ and $c/c^* = 0.38$



(b) 1M PEO, $c/c^* = 0.19$ and $c/c^* = 0.38$



(c) 4M PAM, $c/c^* = 0.19$ and $c/c^* = 0.38$

Figure 2.4: Normalized diameter (D/D_0) of the liquid bridge measured during dripping-onto-substrate extensional rheometry as a function of the time past the critical time (t_c) of transition into the elastocapillary regime (ms), varying solution concentration relative to overlap concentration and number of passes through a pump. The samples' as-prepared molecular weight and backbone were (a) 6M PEO, (b) 1M PEO, and (c) 4M PAM. For each backbone-molecular weight combination, the solutions' reduced concentrations were $c/c^* = 0.19$ (left) and 0.38 (right).

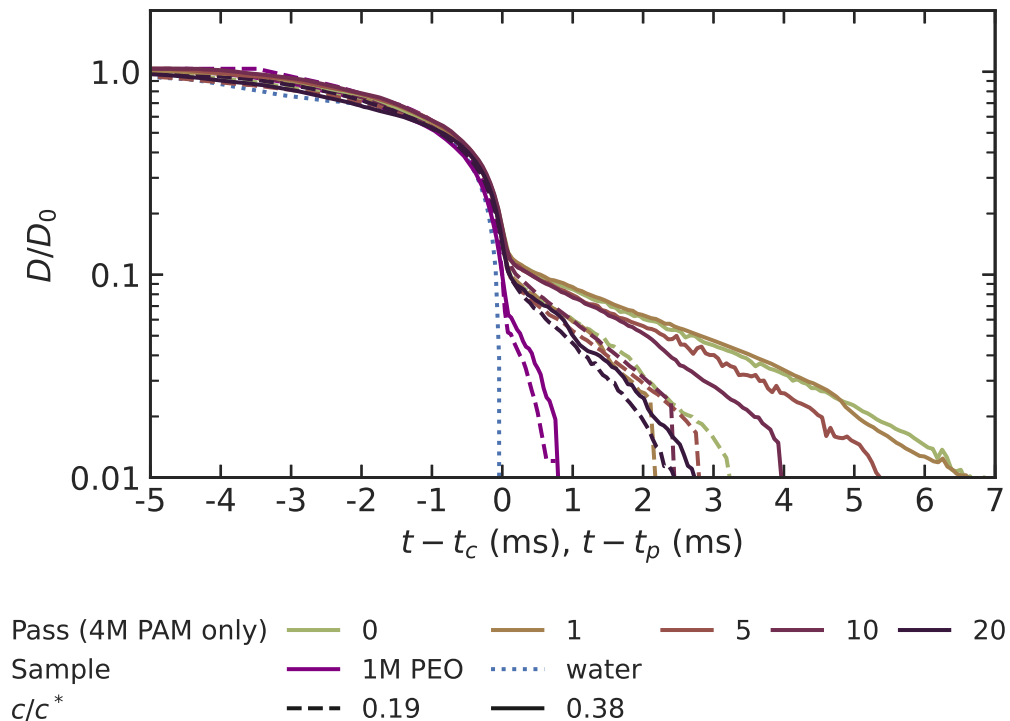


Figure 2.5: Normalized diameter (D/D_0) of the liquid bridge measured during dripping-onto-substrate extensional rheometry as a function of the time (ms) prior to the critical time (t_c) for polymeric samples, 4M PAM (averaged over runs and plotted for each pass) and 1M PEO (averaged over all runs and passes, purple), or pinchoff time (t_p) of the thread of deionized water (averaged over five runs, blue dotted). As-prepared concentrations for 4M PAM and 1M PEO samples were $c/c^* = 0.19$ (dashed) and 0.38 (solid).

Focusing first on the 4M PAM solutions, both the slope of the normalized diameter as a function of time and the EC duration are observed to decrease with successive pass through the pump (Figure 2.5), corresponding to the degradation in molecular weight measured by GPC (Figure 2.3). In contrast, solutions of 1M PEO demonstrate little difference in slope and duration of EC regime with pass number (Figure 2.4(b)), corresponding to the unchanged GPC trace observed for 1M PEO (Figure 2.3).

Fits to the normalized diameter in the elastocapillary regime as described in Appendix A were used to determine the extensional relaxation time (λ_E) for

each specimen (Figure 2.6(a)). The relaxation time of the 6M PEO solutions was observed to rapidly drop with pass number for both concentrations. The relaxation time of the 4M PAM solutions was observed to decrease with pass number and converge to a similar value for both concentrations and the lower concentration 6M PEO solution.

Empirically, Robert Learsch observed a power-law dependence of λ_E on M_w (g/mol) and concentration (c , wt %): $\lambda_E \sim M_w^{K_M} c^{K_c}$. Using PAM solutions having M_w in the range 2.3-6.7 Mg/mol (characterized by GPC) and c in the range 0.01-1 wt %, the exponents were found to be $K_{M,PAM} = 3.5$ and $K_{c,PAM} = 0.82$. Using PEO solutions having M_w in the range 0.5-7.3 Mg/mol (characterized by GPC) and c in the range 0.006-2 wt %, the exponents were found to be $K_{M,PEO} = 2.5$ and $K_{c,PEO} = 0.89$. Discussion of the meaning of the molecular weight and concentration exponents is planned to be in the thesis of Robert Learsch.

By using the empirical power-law relationship for λ_E , I define an effective molecular weight for a given solution as the calculated molecular weight corresponding to the measured relaxation time and concentration. I evaluated the ratio of effective molecular weight at pass i to the starting effective molecular weight ($M_{eff,i}/M_{eff,0}$, dimensionless) for given concentration using Equation 2.3.

$$\frac{M_{eff,i}}{M_{eff,0}} = \left(\frac{\lambda_{E,i}}{\lambda_{E,0}} \right)^{1/K_M} \quad (2.3)$$

For solutions of 4M PAM and 6M PEO that were characterized by both GPC and DoSER, $M_{eff,i}/M_{eff,0}$ correlated with $M_{w,i}/M_{w,0}$ found via GPC, with a correlation of 0.96 (Figure 2.6(c)).

Additional measurements of D/D_0 were performed for solutions undergoing pumping with as-prepared molecular weights and backbones of 6.7M PAM

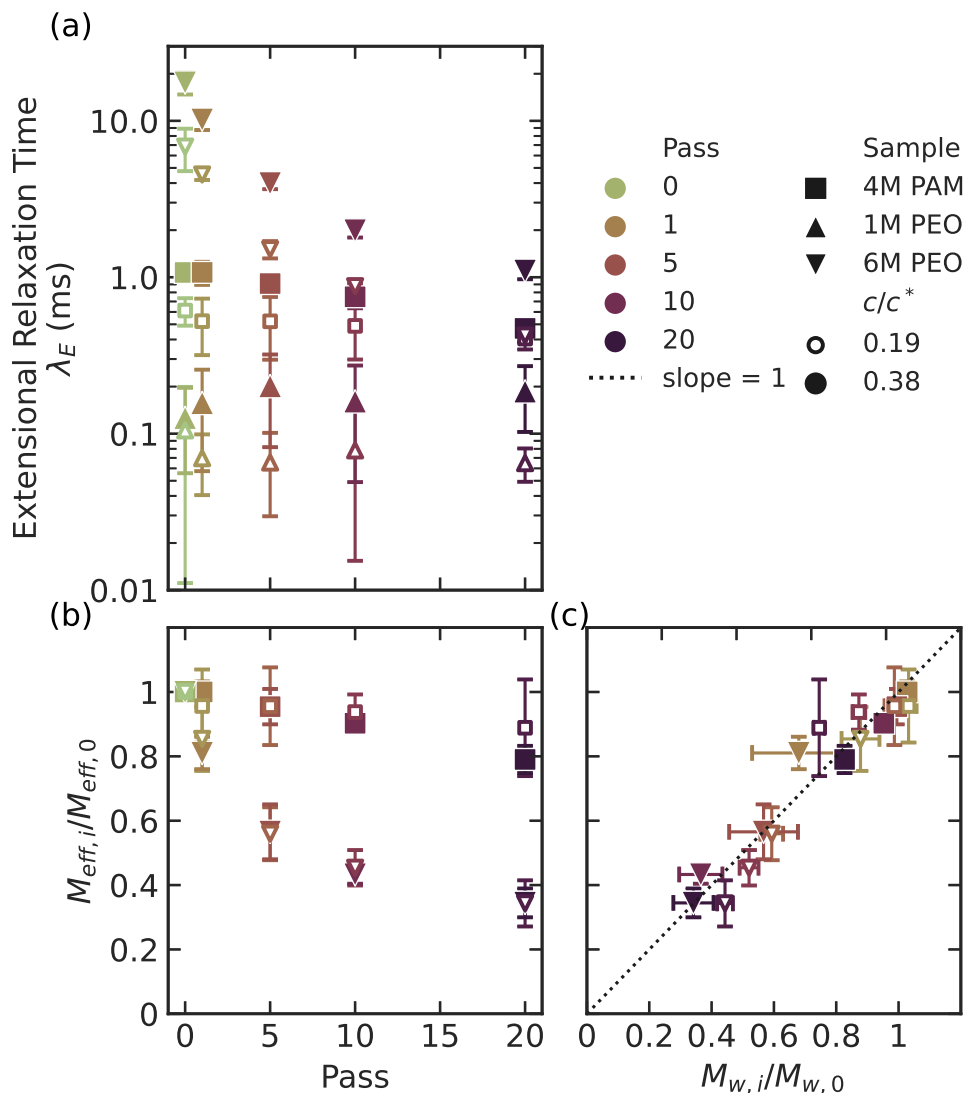
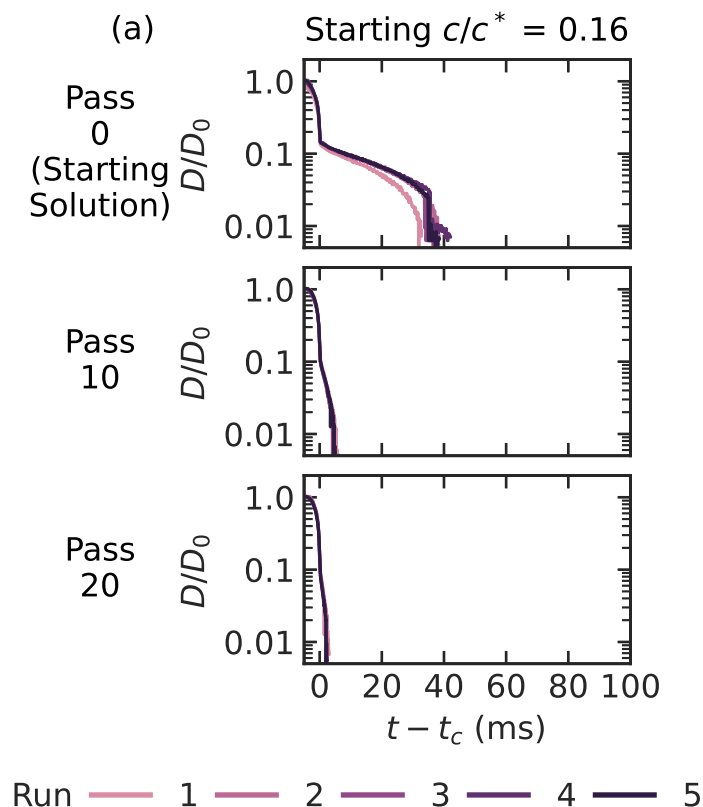
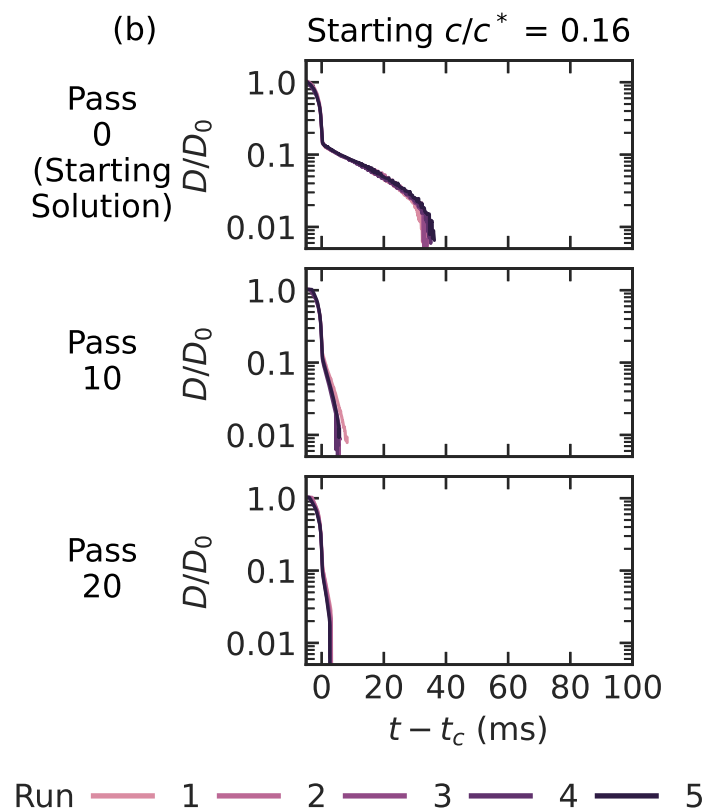


Figure 2.6: Changes with passes through a pump of sample solutions with as-prepared molecular weight and backbone of 4M PAM, 1M PEO, 6M PEO at as-prepared reduced concentrations of $c/c^* = 0.19$ and 0.38 . (a) Extensional relaxation time (λ_E , ms) as a function of passes. (b) Ratio of effective molecular weight of degraded samples to initial effective molecular weight as a function of pass ($M_{eff,i}/M_{eff,0}$), given observed extensional relaxation time from (a) using Equation 2.3, assuming a constant total concentration of the solution. (c) Effective molecular weight ratio ($M_{eff,i}/M_{eff,0}$) from (b) versus measured molecular weight ratio $M_{w,i}/M_{w,0}$ from GPC measurements (Figure 2.3). Dotted line with slope of 1 to guide the eye. In all plots, vertical error bars represent 95% confidence intervals, representing run-to-run variation in DoSER measurements (fitting errors are substantially smaller). Horizontal error bars in (c) represent the statistical standard deviation from propagation of uncertainty of weight-average molecular weight as determined in ASTRA GPC software. In each case, where error bars are not visible, the corresponding interval is within symbol size.

(a) 6M PEO, $c/c^* = 0.16$

(substantially longer than 4M PAM above) and 6M PEO (same PEO as above), with as-prepared reduced concentration of 0.16, lower than the 0.19 above (Figures 2.7 and 2.8). Aliquots were collected and measured for the as-prepared solutions and after pass $i = 10$ and 20. Corresponding GPC measurements were attempted but were not included due to substantial issues with chromatogram spikes that thwarted our ability to meaningfully interpret the results.

As noted above, the inertio-capillary regime corresponded to that of water for all specimens. The elastocapillary behavior observed for 6M PEO at $c/c^*=0.16$ was very similar to the same polymer at $c/c^*=0.19$ (compare Figures 2.4a and 2.7a; open downward triangles from Figure 2.6(a) are repeated in Figure 2.8). The population of longer chains in 6.7M PAM correlate with greater decrease in λ_E at 10 and 20 passes compared to observations for 4M PAM (Figure 2.6).



(b) 6.7M PAM, $c/c^* = 0.16$

Figure 2.7: Normalized diameter (D/D_0) of the liquid bridge measured during dripping-onto-substrate extensional rheometry as a function of the time past the critical time of transition into the elastocapillary regime (ms), varying solution concentration relative to overlap concentration and number of passes through a pump. The samples' as-prepared weight-average molecular weight and backbone were (a) 6.7M PAM and (b) 6M PEO. For each backbone-molecular weight combination, the as-prepared solution reduced concentration was c/c^* of 0.16.

The duration of the elastocapillary regime and the extensional relaxation times were similar for PAM and PEO of similar molecular weights, despite PEO's greater fully extended length ($\sim 190,000$ BBA for 6.7M PAM and $\sim 410,000$ BBA for 6M PEO) (Figure 2.4a). The two polymers degraded in extensional relaxation time similarly as a function of pass (Figure 2.8(a)). As a result, because of the smaller exponent relating relaxation time to effective molecular weight for PAM relative to PEO (compare the resulting exponent of $(1/3.5)$ for PAM to $(1/2.6)$ for PEO in Equation 2.3), the effective molecular weight stayed at a higher value for the 6.7M PAM compared to 6M PEO and reached a similar value to the 4M PAM after 20 passes (3.3M for 6.7M PAM, 3.1M for 4M PAM, 2M for 6M PEO) (Figure 2.8(b)).

2.4 Discussion

Role of Solvent Quality in Chain Scission

The solvent quality at 15 °C for deionized water of PAM appears to be slightly lower than that of PEO based on the measured intrinsic viscosities and the Kuhn-Mark-Houwink-Sakurada fits obtained, indicating that we should expect the PAM chains to be slightly less swollen; water is not as good a solvent for PAM as it is for PEO. As the literature results for PAM vary in their reported values for a , and little to no data are available for either backbone at our temperature and molecular weight range of interest, it is difficult to evaluate the validity of the fit values of a with direct literature comparisons; although our values are within the ranges found in the literature (Table 2.3). Using the relationships discussed in Chapter 1 for the relationship between the Flory exponent ν and a , $\nu = 0.54$ for PAM in water and 0.57 for PEO in water ($\nu = 0.5$ is a theta solvent and $\nu = 0.6$ is a good solvent).

Overlap concentrations of PAM and low and high dispersity PEO as a func-

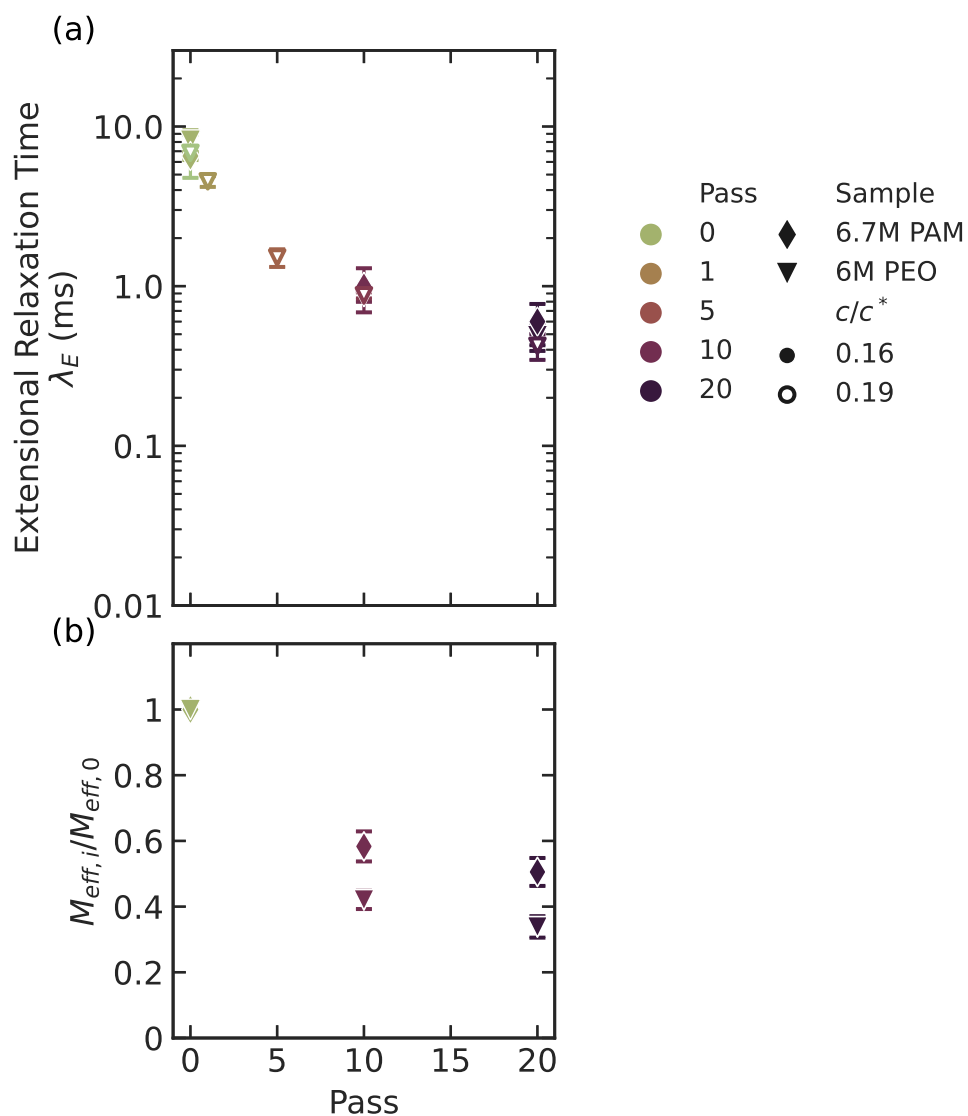


Figure 2.8: Changes with passes through a pump of sample solutions with as-prepared molecular weight and backbone of 6.7M PAM and 6M PEO at an as-prepared reduced concentration of $c/c^* = 0.16$. (a) Extensional relaxation time (λ_E , ms) as a function of passes (open downward triangles are for 6M PEO at $c/c^* = 0.19$, repeated from Figure 2.6(a)). (b) Ratio of effective molecular weight of degraded samples to initial effective molecular weight ($M_{eff,i}/M_{eff,0}$) as a function of pass, given observed extensional relaxation time from (a) using Equation 2.3, assuming a constant concentration of the solution. Vertical error bars represent 95% confidence intervals representing run-to-run variation in DoSER measurements (fitting errors are substantially smaller). Where error bars are not visible, the interval is within symbol size.

tion of weight-average backbone atoms appear to fall along similar curves (Figure 2.2). Normalizing overlap behavior using the weight-average rather than number-average is supported by literature as a method of reducing dependence on dispersity.²⁶ Using backbone atoms allows comparison of the two backbones on the basis of length, removing the differences in molecular weight due to PAM's side groups. Matching PAM and PEO samples on the basis of Kuhn steps also led to similar overlap concentrations—the 4M PAM and 1M PEO used in the chain scission experiments both had overlap concentrations of 0.16 wt %.

The extensional results presented here for undegraded solutions of long PAM and PEO below their respective overlap concentrations agree with literature discussions of different dilution regimes for shear versus extension^{45,46}—even below c^* , the extensional relaxation time demonstrates concentration dependence, indicating interchain interaction in extension even in the dilute regime for shear. I observed similar extensional relaxation times for the PAM and PEO at close molecular weights (6.7M and 6M respectively), despite PAM's fewer backbone atoms per molecular weight and the measured lower solvent quality. When comparing similar equilibrium dimensions, the 4M PAM and 1M PEO have matched Kuhn steps and overlap concentrations, yet the 4M PAM solutions demonstrated relaxation times of 6-8 times that of the 1M PEO at the same concentrations (and reduced concentrations). The combination of these results point towards a picture that the extensional behavior observed in capillary-breakup rheometry is not primarily a function of the equilibrium or shear dimensions of the polymer, but rather the dimensions of the extended chain, both in length and diameter. Dinic and Sharma proposed that differences in chain packing, flexibility, and extensibility all contribute to the observed differences in capillary-breakup behavior of hydroxyethyl cellulose

(a semi-flexible polysaccharide) compared to PEO.⁴⁵ In this work, PAM and PEO are much more similar in each of those proposed parameters due to their similar nature as flexible, synthetic polymers, despite some difference in solvent quality; yet the changes in behavior are still apparent and further support that the drag force on the extended backbone is important to understanding extensional behavior.⁴⁵ The role of solvent quality in extension is discussed further in Chapter 4 for polycyclooctadiene in hydrocarbon solvents.

In chain scission experiments, poorer solvent quality has been shown to result in more degradation.^{38,50-52} Here, the effects of water as poorer solvent for PAM are coupled with differences in drag due to side groups. The combination of these factors is discussed in “Chain Scission Thresholds” below.

Characterizing Chain Scission

Gel permeation chromatography (GPC) has been the primary method of characterizing chain scission in prior studies because of its ability to capture the distribution of molecular weights generated in chain scission events. Researchers have sought equivalents for GPC measurements—for example, Nguyen, et al. proposed using birefringence to characterize molecular weight distributions of extending polymers during flow, but faced obstacles due to peak spreading and noise.⁵³ Additional methods of probing the molecular weight post-scission are advantageous for scenarios where GPC alone may not be an accurate method of characterizing the sample, such as in associative polymers or with backbones with solubility and aggregation issues.

High molecular weight PEO posed challenges for GPC characterization in this study. I observed low mass recovery ($\sim 50\%$ or less) and increased column pressure pointed towards loss of material to the column, which I expect resulted in unreliable molecular weight distributions. Material staying in the

column can damage the instrument due to increased need for higher pressures and can contaminate future measurements, making running high molecular weight PEO through the instrument undesirable. Additionally, even at very low concentrations and with use of a 0.45 μm syringe filter, the light scattering chromatogram had high signal “spikes” that were reduced, but not eliminated, with lowering injected concentration, which indicated highly scattering inclusions. Lowering the concentration, however, diminished the differential refractive index signal available for analysis, contributing to uncertainty in molecular weight estimates.

Combining the more reliable measurements from GPC of 4M PAM with the estimates of the 6M PEO results, I compared the GPC measured molecular weights to effective molecular weights estimated from the extensional relaxation time results (Figure 2.6(c)). The ratios of effective molecular weight and measured weight-average molecular weight to their respective starting values were highly correlated (correlation 0.96; a correlation of 1 would indicate a perfectly 1:1 linear relationship), indicating that we can use our relaxation time estimates of effective molecular weight as a reliable estimator of the molecular weight degradation that has occurred in the solution.

Utilizing extensional rheology as our primary tool for assessing chain scission misses out on the detailed molecular weight distribution, but particularly where GPC is not a reliable measuring device, it is a relatively easy and consistent way of revealing how much a solution has degraded. Extensional behavior is also of particular interest for our applications—as discussed in detail in Chapter 1, the extensional properties of the solution control drag reduction, drop impact, and drop size—and so measuring that behavior directly characterizes the most directly relevant effects of chain scission.

Chain Scission Thresholds

The 6M PEO, in comparison with both the 4M and the 6.7M PAM samples, underwent substantially more degradation during pumping as observed through the change in effective molecular weight (see Figures 2.6 and 2.8). The 1M PEO samples ($\sim 68,000$ BBA), which had approximately the sample number of Kuhn steps and overlap concentration as the 4M PAM ($\sim 120,000$ BBA), did not undergo statistically significant degradation as measured by either GPC or extensional relaxation time. These features indicated that what determined extensional potency and the potential for chain scission was not the pervaded volume at equilibrium (indicated by c/c^*).

After 20 passes, the 6M PEO solutions prepared at c/c^* at 0.16 and 0.19 and all the observed PAM solutions degraded to extensional relaxation times in the range of 0.4 – 0.6 ms (average 0.48 ms \pm 0.21 ms). Although long PEO started off as a more potent extensional rheological modifier, the rapid degradation of the PEO led to similar values of PAM and PEO extensional relaxation time after scission events. Convergence to similar relaxation times indicated that one backbone was not inherently more resilient under the conditions inside the pump in the frame of post-scission extensional behavior.

The convergence of relaxation times may also indicate the extensional rate experienced during pumping—if the rate of extension inside the pump exceeds the ability of the polymer chains to relax the tension, scission may occur.³⁴ If the extensional rate causing scission goes like $\dot{\epsilon} \sim 1/\lambda_{E,i \rightarrow \infty}$, then we expect the maximum extensional rate in this pump is order 1500-2500 1/s.

Assuming that both backbones experience similar extensional rates in the pump, the effective extended length after scission can be looked at as a measure of the relative drag force on each backbone, based on the turbulent drag

force arguments of Vanapalli et al.²⁹ After 20 passes, both the 6.7M and 4M PAM reached effective molecular weights of approximately 3M as determined from extensional relaxation time; 6M PEO degraded to approximately 2M. These effective molecular weights are equivalent to 85,000 BBA for PAM and 140,000 BBA for PEO. The result is that while the PAM's molecular weight is larger post-scission, its fully extended length is shorter than the degraded PEO. Because PEO's reported force for scission is lower than PAM,²⁹ a shorter length for PAM post-pumping implies that the forces on the PAM chain exceed those on the PEO chains at similar extensional rates. The lower solvent quality for PAM and the increased diameter from the side groups may both be contributing to the increased force on the backbone from the surrounding fluid during pumping. The effects of backbone identity on drag reduction and chain scission in turbulent flow is discussed further in Chapter 3.

Degradation experiments by Hojin Kim and extensional measurements by Robert Learsch using a terpyridene-ended telechelic PAM (TPAM) with nickel ions as a water-soluble megasupramolecule demonstrated corresponding behavior. A 0.1 wt% solution of 800 kg/mol TPAM without nickel had an extensional relaxation time of 0.2 ms, below the threshold extensional relaxation time determined in these experiments, while adding one nickel for every two terpyridene end-groups led to a relaxation time of 4.5 ms, above the threshold where degradation was experienced by the homopolymer PAM and PEO. After 20 passes through the same pump, the TPAM-nickel solution did not change in molecular weight as measured by GPC.⁵⁴

2.5 Conclusion

Looking at post-scission polymer lengths measured through both extension and GPC, PAM is not inherently more resistant to mechanical scission than

PEO, even if its backbone itself can withstand a higher force.²⁹ Indeed, PAM degraded to smaller number of backbone atoms (i.e., shorter fully extended lengths) compared to the PEO samples after 20 passes. After scission, however, PAM and PEO's similar extensional relaxation times mean that they have similar potency in the applications of interest—mist control, drag reduction, and droplet impact. Due to the additional issues with PEO—relative vulnerability to chemical degradation due to light and heat, aggregation issues during dissolution and in GPC measurements—PAM becomes a more attractive backbone option because it can comparably perform in extension after scission, despite a smaller effective length post-degradation.

By looking at the extensional properties of polymers pre- and post-scission instead of molecular weight alone, our understanding of additives moves to be more backbone-agnostic. Rather than constraining choices of polymer and concentration to homopolymer solutions previously studied by the literature, or requiring that the exact extension rates inside the equipment are known, these results suggest a design process and engineering criteria for an associative polymer additive. First, one could run a generic polymer solution through the rigors expected of the final solution (a worst-case scenario pump, for example) to characterize the maximum extensional relaxation time that survives. After knowing the maximum that survives, the target extensional relaxation time for a disassociated unimer at the desired concentration should be a safety margin below that maximum, such that the unimer backbone itself will not break in the flow. Thus, if designed to meet this target, the resulting associative additive should survive until their opportunity to act on their intended flows—as rheological modifiers in pipeline flows, mists, and droplets.

References

- [1] W. Wirth, S. Storp, and W. Jacobsen. “Mechanisms Controlling Leaf Retention of Agricultural Spray Solutions”. In: *Pesticide Science* 33.4 (1991), pp. 411–420.
- [2] V. Bergeron et al. “Controlling Droplet Deposition with Polymer Additives”. In: *Nature* 405.6788 (June 2000), pp. 772–775. ISSN: 0028-0836, 1476-4687. DOI: 10.1038/35015525. URL: <http://www.nature.com/articles/35015525> (visited on 08/05/2020).
- [3] T. Holmes, E. Nielsen, and L. Lee. “Managing Groundwater Contamination In Rural Areas”. In: (), p. 9.
- [4] R. Peshin and A. K. Dhawan, eds. *Integrated Pest Management: Dissemination and Impact*. Dordrecht: Springer, 2009. 1 p. ISBN: 978-1-4020-8991-6.
- [5] *USGS FS-122-96: Pesticides in Public Supply Wells of Washington State*. URL: <https://wa.water.usgs.gov/pubs/fs/fs122-96/> (visited on 03/24/2022).
- [6] A. S. Felsot et al. “Agrochemical Spray Drift; Assessment and Mitigation—A Review*”. In: *Journal of Environmental Science and Health, Part B* 46.1 (Dec. 30, 2010), pp. 1–23. ISSN: 0360-1234, 1532-4109. DOI: 10.1080/03601234.2010.515161. URL: <http://www.tandfonline.com/doi/abs/10.1080/03601234.2010.515161> (visited on 03/24/2022).
- [7] R. W. Lewis et al. “Polymeric Drift Control Adjuvants for Agricultural Spraying”. In: *Macromolecular Chemistry and Physics* 217.20 (Oct. 2016), pp. 2223–2242. ISSN: 10221352. DOI: 10.1002/macp.201600139. URL: <https://onlinelibrary.wiley.com/doi/10.1002/macp.201600139> (visited on 03/23/2022).
- [8] E. Hilz. “Spray Drift Review: The Extent to Which a Formulation Can Contribute to Spray Drift Reduction”. In: *Crop Protection* (2013), p. 9.
- [9] M. Xu et al. “Quantifying the Effect of Extensional Rheology on the Retention of Agricultural Sprays”. In: *Physics of Fluids* 33.3 (Mar. 1, 2021), p. 032107. ISSN: 1070-6631, 1089-7666. DOI: 10.1063/5.0038391. URL: <https://aip.scitation.org/doi/10.1063/5.0038391> (visited on 03/15/2021).
- [10] Y. Yeong, J. Burton, and E. Loth. “Drop Impact and Rebound Dynamics on an Inclined Superhydrophobic Surface”. In: *Langmuir* 30 (2014), pp. 12027–12038. DOI: 10.1021/la502500z.
- [11] V. Tirtaatmadja, G. H. McKinley, and J. J. Cooper-White. “Drop Formation and Breakup of Low Viscosity Elastic Fluids: Effects of Molecular Weight and Concentration”. In: *Physics of Fluids* 18.4 (Apr. 2006),

- p. 043101. ISSN: 1070-6631, 1089-7666. DOI: 10.1063/1.2190469. URL: <http://aip.scitation.org/doi/10.1063/1.2190469> (visited on 08/14/2017).
- [12] Y. Song et al. “The Use of Folate/Zinc Supramolecular Hydrogels to Increase Droplet Deposition on *Chenopodium Album* L. Leaves”. In: *ACS Sustainable Chemistry & Engineering* 8.34 (Aug. 31, 2020), pp. 12911–12919. ISSN: 2168-0485, 2168-0485. DOI: 10.1021/acssuschemeng.0c03396. URL: <https://pubs.acs.org/doi/10.1021/acssuschemeng.0c03396> (visited on 09/17/2020).
- [13] M. Song et al. “Controlling Liquid Splash on Superhydrophobic Surfaces by a Vesicle Surfactant”. In: *Science Advances* 3.3 (Mar. 2017), e1602188. ISSN: 2375-2548. DOI: 10.1126/sciadv.1602188. URL: <https://advances.sciencemag.org/lookup/doi/10.1126/sciadv.1602188> (visited on 09/17/2020).
- [14] M. I. Smith and V. Bertola. “Effect of Polymer Additives on the Wetting of Impacting Droplets”. In: *Physical Review Letters* 104.15 (Apr. 15, 2010). ISSN: 0031-9007, 1079-7114. DOI: 10.1103/PhysRevLett.104.154502. URL: <https://link.aps.org/doi/10.1103/PhysRevLett.104.154502> (visited on 08/05/2020).
- [15] R. P. Mun, J. A. Byars, and D. V. Boger. “The Effects of Polymer Concentration and Molecular Weight on the Breakup of Laminar Capillary Jets”. In: (1998), p. 13.
- [16] B. Keshavarz et al. “Studying the Effects of Elongational Properties on Atomization of Weakly Viscoelastic Solutions Using Rayleigh Ohnesorge Jetting Extensional Rheometry (ROJER)”. In: *Journal of Non-Newtonian Fluid Mechanics* 222 (Aug. 2015), pp. 171–189. ISSN: 03770257. DOI: 10.1016/j.jnnfm.2014.11.004. URL: <http://linkinghub.elsevier.com/retrieve/pii/S0377025714002055> (visited on 01/06/2017).
- [17] P. S. Virk. “Drag Reduction Fundamentals”. In: *AIChE Journal* 21.4 (July 1975), pp. 625–656.
- [18] S. A. Vanapalli, M. T. Islam, and M. J. Solomon. “Scission-Induced Bounds on Maximum Polymer Drag Reduction in Turbulent Flow”. In: *Physics of Fluids* 17.9 (2005), p. 095108. ISSN: 10706631. DOI: 10.1063/1.2042489. URL: <http://scitation.aip.org/content/aip/journal/pof2/17/9/10.1063/1.2042489> (visited on 05/05/2016).
- [19] A. Somervaille, G. Betts, and C. F. I. Grains Research and Development Corporation (Australia). *Adjuvants: Oils, Surfactants and Other Additives for Farm Chemicals*. Kingston, ACT: Grains Research & Development Corporation, 2011. ISBN: 978-1-921779-32-9.

- [20] H. Zhu et al. “Effects of Polymer Composition and Viscosity on Droplet Size of Recirculated Spray Solutions”. In: *Journal of Agricultural Engineering Research* 67.1 (May 1997), pp. 35–45. ISSN: 00218634. DOI: 10.1006/jaer.1997.0151. URL: <https://linkinghub.elsevier.com/retrieve/pii/S0021863497901517> (visited on 03/23/2022).
- [21] v. W. Scholtan. “Molekulargewichtsbestimmung von Polyacrylamid mittels der Ultrazentrifuge”. In: *Die Makromolekulare Chemie* 14.1 (1954), pp. 169–178. ISSN: 0025116X, 0025116X. DOI: 10.1002/macp.1954.020140113. URL: <http://doi.wiley.com/10.1002/macp.1954.020140113> (visited on 02/04/2021).
- [22] E. Collinson, F. S. Dainton, and G. S. McNaughton. “The Polymerization of Acrylamide in Aqueous Solution. Part 2.—The Effect of Ferric Perchlorate on the X- and γ -Ray Initiated Reaction”. In: *Transactions of the Faraday Society* 53.0 (1957), pp. 489–498. ISSN: 0014-7672. DOI: 10.1039/TF9575300489. URL: <http://dx.doi.org/10.1039/TF9575300489>.
- [23] G. Misra and S. Bhattacharya. “Determination of the Molecular Weight of Polyacrylamide Fractions by Osmometry”. In: *European Polymer Journal* 15.2 (Jan. 1979), pp. 125–128. ISSN: 00143057. DOI: 10.1016/0014-3057(79)90196-4. URL: <https://linkinghub.elsevier.com/retrieve/pii/0014305779901964> (visited on 02/04/2021).
- [24] P. Gregory and M. B. Huglin. “Viscosity of Aqueous and Alkaline Solutions of Poly(Ethylene Oxide)”. In: *Die Makromolekulare Chemie* 187.7 (July 1986), pp. 1745–1755. ISSN: 0025116X, 0025116X. DOI: 10.1002/macp.1986.021870718. URL: <http://doi.wiley.com/10.1002/macp.1986.021870718> (visited on 02/03/2021).
- [25] F. E. Bailey, J. L. Kucera, and L. G. Imhof. “Molecular Weight Relations of Poly(Ethylene Oxide)”. In: *Journal of Polymer Science* 32.125 (Nov. 1958), pp. 517–518. ISSN: 00223832, 15426238. DOI: 10.1002/pol.1958.1203212522. URL: <http://doi.wiley.com/10.1002/pol.1958.1203212522> (visited on 02/04/2021).
- [26] M. Bohdanecký, V. Petrus, and B. Sedláček. “Estimation of the Characteristic Ratio of Polyacrylamide in Water and in a Mixed Theta-solvent”. In: *Die Makromolekulare Chemie* 184.10 (Oct. 1983), pp. 2061–2073. ISSN: 0025116X, 0025116X. DOI: 10.1002/macp.1983.021841011. URL: <http://doi.wiley.com/10.1002/macp.1983.021841011> (visited on 02/04/2021).
- [27] Chemical Retrieval on the Web. *Characteristic Ratio*. Polymer Database. Mar. 31, 2022. URL: <http://polymerdatabase.com/polymer%20physics/C%20Table%20.html> (visited on 03/31/2022).

- [28] M. Rubinstein and R. H. Colby. *Polymer Physics*. Oxford ; New York: Oxford University Press, 2003. 440 pp. ISBN: 978-0-19-852059-7.
- [29] S. A. Vanapalli, S. L. Ceccio, and M. J. Solomon. “Universal Scaling for Polymer Chain Scission in Turbulence”. In: *Proceedings of the National Academy of Sciences* 103.45 (Nov. 7, 2006), pp. 16660–16665. ISSN: 0027-8424, 1091-6490. DOI: 10.1073/pnas.0607933103. URL: <http://www.pnas.org/cgi/doi/10.1073/pnas.0607933103> (visited on 09/11/2016).
- [30] R. Crooks and D. V. Boger. “Influence of Fluid Elasticity on Drops Impacting on Dry Surfaces”. In: *Journal of Rheology* 44.4 (July 2000), pp. 973–996. ISSN: 0148-6055, 1520-8516. DOI: 10.1122/1.551123. URL: <http://sor.scitation.org/doi/10.1122/1.551123> (visited on 08/05/2020).
- [31] V. Bertola. “An Experimental Study of Bouncing Leidenfrost Drops: Comparison between Newtonian and Viscoelastic Liquids”. In: *International Journal of Heat and Mass Transfer* 52.7-8 (Mar. 2009), pp. 1786–1793. ISSN: 00179310. DOI: 10.1016/j.ijheatmasstransfer.2008.09.028. URL: <https://linkinghub.elsevier.com/retrieve/pii/S0017931008005875> (visited on 08/06/2020).
- [32] V. Bertola. “Effect of Polymer Concentration on the Dynamics of Dilute Polymer Solution Drops Impacting on Heated Surfaces in the Leidenfrost Regime”. In: *Experimental Thermal and Fluid Science* 52 (Jan. 2014), pp. 259–269. ISSN: 08941777. DOI: 10.1016/j.expthermflusci.2013.09.019. URL: <https://linkinghub.elsevier.com/retrieve/pii/S0894177713002306> (visited on 09/02/2020).
- [33] A. Keller and J. A. Odell. “The Extensibility of Macromolecules in Solution; A New Focus for Macromolecular Science”. In: *Colloid & Polymer Science* 263.3 (Mar. 1985), pp. 181–201. ISSN: 0303-402X, 1435-1536. DOI: 10.1007/BF01415506. URL: <http://link.springer.com/10.1007/BF01415506> (visited on 04/06/2022).
- [34] T. Q. Nguyen and H.-H. Kausch. “Chain Scission in Transient Extensional Flow Kinetics and Molecular Weight Dependence”. In: *Journal of non-newtonian fluid mechanics* 30.2-3 (1988), pp. 125–140. URL: <http://www.sciencedirect.com/science/article/pii/0377025788850201> (visited on 09/11/2016).
- [35] H. G. Sim, B. Khomami, and R. Sureshkumar. “Flow-Induced Chain Scission in Dilute Polymer Solutions: Algorithm Development and Results for Scission Dynamics in Elongational Flow”. In: *Journal of Rheology* 51.6 (2007), p. 1223. ISSN: 01486055. DOI: 10.1122/1.2789945. URL: <http://scitation.aip.org/content/sor/journal/jor2/51/6/10.1122/1.2789945> (visited on 08/29/2016).

- [36] J. Dinic et al. “Extensional Relaxation Times of Dilute, Aqueous Polymer Solutions”. In: *ACS Macro Letters* 4.7 (July 21, 2015), pp. 804–808. ISSN: 2161-1653, 2161-1653. DOI: 10.1021/acsmacrolett.5b00393. URL: <http://pubs.acs.org/doi/abs/10.1021/acsmacrolett.5b00393> (visited on 03/17/2016).
- [37] P. Nghe, P. Tabeling, and A. Ajdari. “Flow-Induced Polymer Degradation Probed by a High Throughput Microfluidic Set-Up”. In: *Journal of Non-Newtonian Fluid Mechanics* 165.7 (2010), pp. 313–322. URL: <http://www.sciencedirect.com/science/article/pii/S037702571000008X> (visited on 09/13/2016).
- [38] A. Dupas et al. “Mechanical Degradation Onset of Polyethylene Oxide Used as a Hydrosoluble Model Polymer for Enhanced Oil Recovery”. In: *Oil & Gas Science and Technology – Revue d’IFP Energies nouvelles* 67.6 (Nov. 2012), pp. 931–940. ISSN: 1294-4475, 1953-8189. DOI: 10.2516/ogst/2012028. URL: <http://ogst.ifpenergiesnouvelles.fr/10.2516/ogst/2012028> (visited on 01/15/2019).
- [39] K. Brakstad and C. Rosenkilde. “Modelling Viscosity and Mechanical Degradation of Polyacrylamide Solutions in Porous Media”. In: *All Days. SPE Improved Oil Recovery Conference*. Tulsa, Oklahoma, USA: SPE, Apr. 11, 2016, SPE-179593–MS. DOI: 10.2118/179593–MS. URL: <https://onepetro.org/SPEIOR/proceedings/16IOR/All-16IOR/Tulsa,%20Oklahoma,%20USA/187343> (visited on 03/23/2022).
- [40] S. L. Anna and G. H. McKinley. “Elasto-Capillary Thinning and Breakup of Model Elastic Liquids”. In: *Journal of Rheology* 45.1 (2001), p. 115. ISSN: 01486055. DOI: 10.1122/1.1332389. URL: <http://scitation.aip.org/content/sor/journal/jor2/45/1/10.1122/1.1332389> (visited on 03/22/2016).
- [41] J. Dinic, M. Biagioli, and V. Sharma. “Pinch-off Dynamics and Extensional Relaxation Times of Intrinsically Semi-Dilute Polymer Solutions Characterized by Dripping-onto-Substrate Rheometry”. In: *Journal of Polymer Science Part B: Polymer Physics* 55.22 (Nov. 15, 2017), pp. 1692–1704. ISSN: 08876266. DOI: 10.1002/polb.24388. URL: <http://doi.wiley.com/10.1002/polb.24388> (visited on 03/05/2020).
- [42] J. Dinic, L. N. Jimenez, and V. Sharma. “Pinch-off Dynamics and Dripping-onto-Substrate (DoS) Rheometry of Complex Fluids”. In: *Lab on a Chip* 17.3 (2017), pp. 460–473. ISSN: 1473-0197, 1473-0189. DOI: 10.1039/C6LC01155A. URL: <http://xlink.rsc.org/?DOI=C6LC01155A> (visited on 02/10/2020).
- [43] E. Greiciunas et al. “Design and Operation of a Rayleigh Ohnesorge Jetting Extensional Rheometer (ROJER) to Study Extensional Properties of Low Viscosity Polymer Solutions”. In: *Journal of Rheology* 61.3 (May 2017), pp. 467–476. ISSN: 0148-6055, 1520-8516. DOI: 10.1122/1.

4979099. URL: <http://sor.scitation.org/doi/10.1122/1.4979099> (visited on 03/31/2022).
- [44] J. Dinic and V. Sharma. “Macromolecular Relaxation, Strain, and Extensibility Determine Elastocapillary Thinning and Extensional Viscosity of Polymer Solutions”. In: *Proceedings of the National Academy of Sciences* 116.18 (Apr. 30, 2019), pp. 8766–8774. ISSN: 0027-8424, 1091-6490. DOI: 10.1073/pnas.1820277116. URL: <http://www.pnas.org/lookup/doi/10.1073/pnas.1820277116> (visited on 05/05/2021).
- [45] J. Dinic and V. Sharma. “Flexibility, Extensibility, and Ratio of Kuhn Length to Packing Length Govern the Pinching Dynamics, Coil-Stretch Transition, and Rheology of Polymer Solutions”. In: *Macromolecules* 53.12 (June 23, 2020), pp. 4821–4835. ISSN: 0024-9297, 1520-5835. DOI: 10.1021/acs.macromol.0c00076. URL: <https://pubs.acs.org/doi/10.1021/acs.macromol.0c00076> (visited on 05/05/2021).
- [46] C. Clasen et al. “How Dilute Are Dilute Solutions in Extensional Flows?” In: *Journal of Rheology* 50.6 (Nov. 2006), pp. 849–881. ISSN: 0148-6055, 1520-8516. DOI: 10.1122/1.2357595. URL: <http://sor.scitation.org/doi/10.1122/1.2357595> (visited on 05/14/2021).
- [47] B. Keshavarz and G. H. McKinley. “Micro-Scale Extensional Rheometry Using Hyperbolic Converging/Diverging Channels and Jet Breakup”. In: *Biomicrofluidics* 10.4 (July 2016), p. 043502. ISSN: 1932-1058. DOI: 10.1063/1.4948235. URL: <http://scitation.aip.org/content/aip/journal/bmf/10/4/10.1063/1.4948235> (visited on 10/14/2016).
- [48] R. Learsch. “Investigation in Experimental Conditions and Automation of Dripping-onto-Substrate Rheology”. American Chemical Society Spring Meeting (San Diego, CA). Mar. 23, 2022.
- [49] S. A. Vanapalli. “Polymer Chain Scission in Extensional and Turbulent Flows and Implications for Friction Drag Technologies”. University of Michigan, 2006. 219 pp.
- [50] F. Rodriguez and C. Winding. “Mechanical Degradation of Dilute Polyisobutylene Solutions”. In: *Industrial & Engineering Chemistry* 51.10 (Oct. 1959), pp. 1281–1284. ISSN: 0019-7866, 1541-5724. DOI: 10.1021/ie50598a034. URL: <https://pubs.acs.org/doi/abs/10.1021/ie50598a034> (visited on 04/12/2022).
- [51] Y. Minoura et al. “Degradation of Poly(Ethylene Oxide) by High-Speed Stirring”. In: *Journal of Polymer Science Part A-2: Polymer Physics* 5.1 (Jan. 1967), pp. 125–142. ISSN: 04492978, 15429377. DOI: 10.1002/pol.1967.160050111. URL: <https://onlinelibrary.wiley.com/doi/10.1002/pol.1967.160050111> (visited on 04/12/2022).

- [52] R. E. Harrington and B. H. Zimm. “Degradation of Polymers by Controlled Hydrodynamic Shear ¹”. In: *The Journal of Physical Chemistry* 69.1 (Jan. 1965), pp. 161–175. ISSN: 0022-3654, 1541-5740. DOI: 10.1021/j100885a025. URL: <https://pubs.acs.org/doi/10.1021/j100885a025> (visited on 04/12/2022).
- [53] T. Q. Nguyen, G. Yu, and H.-H. Kausch. “Birefringence of a Polystyrene Solution in Elongational Flow: Effects of Molecular Weight and Solvent Quality”. In: *Macromolecules* 28.14 (July 1995), pp. 4851–4860. ISSN: 0024-9297, 1520-5835. DOI: 10.1021/ma00118a010. URL: <http://pubs.acs.org/doi/abs/10.1021/ma00118a010> (visited on 09/13/2016).
- [54] R. W. Learsch. “Long, Associative, Telechelic Poly(Acrylamide) under Shear and Extensional Flow”. American Chemical Society Spring Meeting (San Diego, CA). Mar. 20, 2022.